# THE PULL-OUT CAPACITY OF MOBILE PLATFORM LEGS FROM SATURATED SILT

## X.W. ZHANG[*], R. UZUOKA[†] AND X.W. TANG[‡]

[*]Dalian University of Technology; The University of Tokushima
No.2 Linggong Road, Ganjingzi District, 116024 Dalian, CHINA
e-mail: zhangxw_11@163.com, Web page: http://www.dlut.edu.cn/en/

[†] The University of Tokushima
2-1 Minamijyousanjima-cho, 770-8506 Tokushima, JAPAN
e-mail: uzuoka@ce.tokushima-u.ac.jp, Web page: http://www.tokushima-u.ac.jp/english/

[‡] Dalian University of Technology
No.2 Linggong Road, Ganjingzi District, 116024 Dalian, CHINA
e-mail: tangxw@dlut.edu.cn, Web page: http://www.dlut.edu.cn/en/

**Key words:** Mobile Platform, Pullout, Suction Force

**Abstract.** Many new types of structures are extensively used in offshore engineering in recent few decades. Such as the mobile platforms, suction caissons, anchors, spudcans, and so on. The capacities of these structures during penetration, operation and remove are crucial issues for engineers. In this paper, the model test and numerical simulation are conducted to estimate the pullout capacity of the mobile platform's leg submerged in saturated silt. The platform's leg is simplified as a square shape with a dimension of 30cm×30cm, while the buried depths are 1cm, 3cm, 5cm, respectively. The modified Cam-Clay model and finite deformation theory are applied in numerical simulation.

We did the short-time pullout in experiment and numerical simulation. The peak pullout force is about 1-4 times larger than the model's weight. The pullout resistance is influenced by the object buried depth, soil property and so on. It is shown that during uplift, the negative pore water pressure under the object provides the main role to the resistance capacity. As the increase of negative pore water pressure and decrease of the soil confining pressure, the soil failure and large deformation happens, then the structure extricates itself from the silt. The numerical result is acceptable to predict the breakout although couldn't simulate the separation of object and soil.

# 1 INTRODUCTION

There are many types of offshore platforms which are extensively used for oil and natural gas extraction. Now, many special platforms are used for turbine installation, sunken ship salvage and so on. For the offshore structures, there are many challenges in geotechnical engineering, such as site investigation, the interaction between the structure and the seabed soil and so on [1]. In this paper, we will focus on a special marine platform, Jack-up platform. Figure 1 shows the Jack-up wind turbine installation platform which works in Nantong City of China.



**Figure 1**: Jack-up wind turbine installation platform (Nantong City, China)

Jack-up platform is a new type and most popular mobile platform in the world. It consists of a buoyant hull and a number of movable legs. The buoyant hull enable the platform to float on the water, while the legs can penetrate into the seabed soil to support the upper platform. This kind of platform can only be placed in relatively shallow water, about less than 100m of water. It can be used as exploratory drilling platform or wind farm service platform.

Jack-up platform has three working process. The first one is penetration. When the jack-up platform arrivals at the working location, the legs will penetrate into the seabed soil by the platform's selfweight and additional water, while the jacking system raises the hull above the water surface with a certain height. Many researchers did research on the penetration process and the capacity of the seabed to support the platform in complicated marine enviroment. Then second one is working. After installation and preloading, the platform can work for construction or salvage. The third one is remove. The jacking system will put down the hull to the water surface and pullout the legs. In this process the pullout force always larger than the legs weight because of the suction force between the seabed and the legs. We will investigate the pullout resistance during the remove of Jack-up platform.

The suction force $F_s$ is defined as the difference between vertical pull force F and the self-weight of leg G. $F_s = F - G$. The suction force is consisted of structure bottom adhesion force, the side friction force and the negative porewater pressure, among which negative porewater pressure is the main factor to the suction force [2]. And the suction force is influenced by many factors such as the shape of the structure, the embedded depth and the seabed soil characteristics. So that, the calculation and the prediction is difficult and complex. Many researchers have done a lot of work in model tests, theory and empirical prediction and numerical simulations ( Finn [3], Sawiciki [4], Purwana [5], Zhou [6] ). And published literature is still relatively scarce.

These suction force should be overcome in order to pullout the platform's legs. Sometimes, the legs are difficult to pullout, or the large impulse force will induce huge damage to the platform and the equipments. This phenomenon is called breakout phenomenon [7, 4]. Chen [8] did a series of centrifuge tests to test the pullout resistance of offshore structure. He found that during remove the structure, the suction force infuence the uplift process. The breakout phenomenon can be divided into short time breakout and long time breakout. As its name suggests, in short time breakout, the vertical force is applied quickly, the object will be pulled out in a short time. In long time breakout, a constant force is applied, as the migration of around water, the object will get extrication in the last, but it will need a longer time. In this paper, the model test and numerical simulation were conducted to predict the peak pullout force and peak suction force in the case of short time pullout. The mechanism of the short time breakout will be discussed.

## 2 EXPERIMENT AND NUMERICAL MODEL

The experiment equipments and numerical model are shown in Figure 2. The platform leg's bottom is simplified as a square with a dimension of 30cm×30cm.
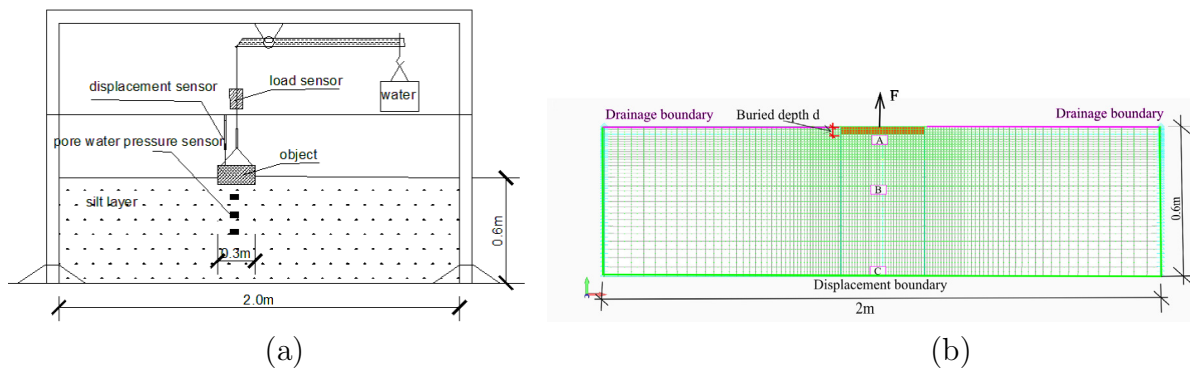


**Figure 2**: (a) Experiment equipment ; (b) Finite element model

### 2.1 Basic condition

The weight of the leg is 103N, while the buried depths are 1cm, 3cm, 5cm respectively. In the experiment, the soil is silt which was excavated from the seabed near Dafeng city

of China. The properties of the silt are shown in Table 1. During the pullout, the displacement, pullout force and the porewater pressure were recorded by the sensors and computer. In numerical simulation, the leg is a rigid body, leg's two sides are free while the bottom is tied with the soil elements. A vertical force with a loading rate of 12N/s is applied on the center of the leg.

**Table 1**: soil property

| Porosity | Intrinsic density | Compression index | Swelling index | Critical stress ratio |
|---|---|---|---|---|
| 0.42 | 2.73 t/m$^3$ | 0.047 | 0.0043 | 1.578 |

In numerical analysis, Al-Shamrani [9] used finite element method to calculate the breakout force with the assumption that no separation of the object and the surrounding soil. Sawiciki [4] and Zhou [6] suggested that the breakout process could be consist of two stages (no gape stage and with gape stage) or three stage (no gape stage,transition stage and with-gap stage). In our experiments, a short time pullout is conducted, which means the leg will be pulled out in a short time. In this case, the pullout time is about dozens of seconds or several minutes, the water and soil migration are not considered. What's more, in our experiment, we found that the stage before the gape emergence is very important. In this stage, the bottom porewater pressure will change form postive to negative, the soil effective stress will decrease and near to zero. After the gape emergence, plenty of water will flow into the gape, the leg will be pulled out in a short time.

As we know, the bubble or the gape is generated in saturated soil when the negative pore water pressure is less than -100kPa (one atmos). Actually, the negative pore water pressure is larger than that value in our experiment. So that, a no gape model is assumed in this paper. To simulate the soil property, the modified cam-clay model is applied to simulate the elasto-plastic behavious in the numerical analysis.

## 2.2 Governing equations

According to Uzuoka [10] porous media theory and finite strain analysis, we used quasi-static analyses and established mass and momentum balance equations for the saturated soil. The momentum balance equation for total mixture is obtained as:

$$\text{div}\left(\boldsymbol{\sigma}' - p^{\text{w}}\boldsymbol{I}\right) + \rho\boldsymbol{b} = 0 \tag{1}$$

Where, $\boldsymbol{\sigma}'$ is Cauchy effective stress tensor, $p^{\text{w}}$ is pore water pressure, $\boldsymbol{I}$ is the second-order identity tensor (Kronecker delta function), $\rho$ is density of the mixture, $\boldsymbol{b}$ is the body force vector. The mass and momentum balance equation for pore water is obtained as:

$$\frac{n\rho^{\text{wR}}}{K^{\text{w}}}\frac{D^{\text{s}}p^{\text{w}}}{Dt} + \rho^{\text{wR}}\text{div}\,\boldsymbol{v}^{\text{s}} + \text{div}\left\{\frac{k^{\text{ws}}}{g}(-\text{grad}\,p^{\text{w}} + \rho^{\text{wR}}\boldsymbol{b})\right\} = 0 \tag{2}$$

Where, n is the porosity, $\rho^{\mathrm{wR}}$ is intrinsic density of fluid, $K^{\mathrm{w}}$ is water bulk modulus, $\boldsymbol{v}^{\mathrm{s}}$ is velocity of soil skeleton, $k^{\mathrm{ws}}$ is permeability coefficients of pore water, g is gravity acceleration.

Then, the finite element method is used for the spatial discretization. Using conventional Galerkin method, the weak form of equation (1) is obtained as

$$\delta w^{\mathrm{s}} = \int_{B^{\mathrm{s}}} \delta \boldsymbol{d}^{\mathrm{s}} : \boldsymbol{\sigma}' dv - \int_{B^{\mathrm{s}}} p^{\mathrm{w}} \mathrm{div}\, \delta \boldsymbol{v}^{\mathrm{s}} dv - \int_{B^{\mathrm{s}}} \rho \delta \boldsymbol{v}^{\mathrm{s}} \cdot \boldsymbol{b} dv - \int_{\partial B^{\mathrm{s}}_{\mathrm{t}}} \delta \boldsymbol{v}^{\mathrm{s}} \cdot \bar{\boldsymbol{t}} da = 0. \quad (3)$$

The weak form of equation (2) is

$$\delta w^{\mathrm{w}} = \int_{B^{\mathrm{s}}} \delta p^{\mathrm{w}} \frac{n s^{\mathrm{w}} \rho^{\mathrm{wR}}}{K^{\mathrm{w}}} \frac{D^{\mathrm{s}} p^{\mathrm{w}}}{Dt} dv + \int_{B^{\mathrm{s}}} \delta p^{\mathrm{w}} \rho^{\mathrm{wR}} \mathrm{div}\, \boldsymbol{v}^{\mathrm{s}} dv$$
$$- \int_{B^{\mathrm{s}}} \mathrm{grad}\, \delta p^{\mathrm{w}} \cdot \left\{ \frac{k^{\mathrm{ws}}}{g} (-\mathrm{grad}\, p^{\mathrm{w}} + \rho^{\mathrm{wR}} \boldsymbol{b}) \right\} dv$$
$$+ \int_{\partial B^{\mathrm{s}}_{\mathrm{wq}}} \delta p^{\mathrm{w}} \bar{q}^{\mathrm{w}} da = 0. \quad (4)$$

Where, $B^{\mathrm{s}}$ is body area, $\partial B^{\mathrm{s}}_{\mathrm{t}}$ and $\partial B^{\mathrm{s}}_{\mathrm{wp}}$ are natural boundary, $\bar{\boldsymbol{t}}$ is the prescribed traction vector at $\partial B^{\mathrm{s}}_{\mathrm{t}}$, $\bar{q}^{\mathrm{w}}$ is the prescribed mass flux on a unit at $\partial B^{\mathrm{s}}_{\mathrm{wp}}$. The following equation (5) shows the linearized formulations of the weak forms in Newton-Raphson scheme.

$$D\delta w^{\mathrm{s}}[\Delta \boldsymbol{v}^{\mathrm{s}}] + D\delta w^{\mathrm{s}}[\Delta \dot{p}^{\mathrm{w}}] = -\delta w^{\mathrm{s}}_k$$
$$D\delta w^{\mathrm{w}}[\Delta \boldsymbol{v}^{\mathrm{s}}] + D\delta w^{\mathrm{w}}[\Delta \dot{p}^{\mathrm{w}}] = -\delta w^{\mathrm{w}}_k \quad (5)$$

Where, $\Delta \boldsymbol{v}^{\mathrm{s}}$ and $\Delta \dot{p}^{\mathrm{w}}$ are the variations at the current iterative step $k+1$. $\delta w^{\mathrm{s}}_k$ and $\delta w^{\mathrm{w}}_k$ are the weak form of equation (1) and equation (2) at the previous iterative step $k$. $D\square[\Delta\bullet]$ denotes the directional derivative of $\square$ with respect to $\bullet$. The solutions at the current iterative step $k+1$ are obtained as

$$\boldsymbol{v}^{\mathrm{s}}_{k+1} = \boldsymbol{v}^{\mathrm{s}}_k + \Delta \boldsymbol{v}^{\mathrm{s}}$$
$$\dot{p}^{\mathrm{w}}_{k+1} = \dot{p}^{\mathrm{w}}_k + \Delta \dot{p}^{\mathrm{w}} \quad (6)$$

The iteration continues until the norms of the residual vectors of $\delta w^{\mathrm{s}}_k$ and $\delta w^{\mathrm{w}}_k$ are smaller than a specified error tolerance. In quasi-static analyses, only the velocity components are considered. The displacement of the soil skeleton and the pore water pressure of element are expressed as:

$$\boldsymbol{u}^{\mathrm{s}} = \boldsymbol{u}^{\mathrm{s}}_t + (1-\gamma)\Delta t\, \boldsymbol{v}^{\mathrm{s}}_t + \gamma \Delta t\, \boldsymbol{v}^{\mathrm{s}} \quad (7)$$
$$p^{\mathrm{w}} = p^{\mathrm{w}}_t + (1-\gamma)\Delta t\, \dot{p}^{\mathrm{w}}_t + \gamma \Delta t\, \dot{p}^{\mathrm{w}} \quad (8)$$

Here, $\gamma$ is the parameter in quasi-static analysis.

## 3  RESULTS OF EXPERIMENT AND NUMERICAL SIMULATION

In short time pullout, we will apply a linear loading with a rate of 12N/s, In this case, the pullout time is about dozens of seconds, the soil can be considered as in undrained condition. We will discuss the results about relationship between displacement and vertical force. Then, the transformation of pore water pressure and suction force will be presented.

### 3.1  Displacement-force relationship

Figure 3 shows the relationship between vertical pull force and leg's vertical displacemetn in different buried depth. From this figure, we can see that in different buried depth, the pullout force is different. As increase of buried depth d, the pullout force becomes larger. At the beginning, the vertical displacement increase slowly, while the vertical force has to overcome the object's weight and the suction force. Then, the displacement increase rapidly which is induced by the large soil deformation and partial soil failure.
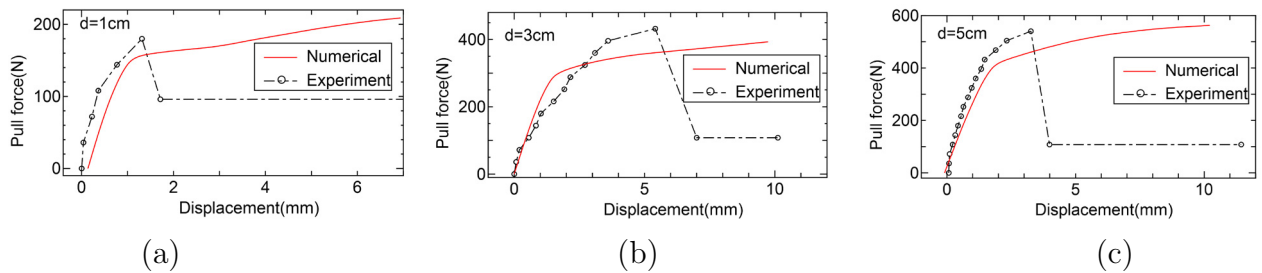


Figure 3: The relationship of displacement and pull force (a)buried deppth d=1cm ; (b) buried deppth d=3cm ; (c) buried deppth d=5cm

In experiment, the pull force decrease rapidly after reach the peak pullout force, that because of the disappear of resistance after the separation between object and the soil, the load sensor can only record the inertial force of the object in the last. In numerical simulation, we can see the obvious turning point. After that point, the soil became weak, which means small force increment will induce large deformation. So, we get the similar phenomenon both from experiment and numerical simulation, that the object has large and rapid displacement in the last. For practical engineering, in the moment of separation, a large impulse force will be generated and it will cause unimaginable damage to the platform.

### 3.2  The suction force

To pull out the object from the seabed soil, the pullout force should be larger than the object's weight. In table 2, it shows the peak pullout force and peak suction force.

**Table 2**: Suction force

| Buried depth | selfweight | Peak pullout force | | Peak suction force | |
|---|---|---|---|---|---|
| | | Experiment | Numerical | Experiment | Numerical |
| 1cm | 103N | 180N | 209N | 77N | 106N |
| 3cm | 103N | 432N | 392N | 329N | 289N |
| 5cm | 103N | 540N | 560N | 437N | 455N |

We define the suction force $F_s$ equals to the difference between vertical force $F$ and the effective selfweight $G$. $F_s = F - G$. Clearly, the peak pullout force is larger than the object's weight. The experiment results and the numerical simulation have the same trend although a little difference exist.

## 3.3 Pore water pressure response

From the model test and numerical simulation, the time history of pore water pressure and the effective stress under the bottom of the object are shown in figure 4.
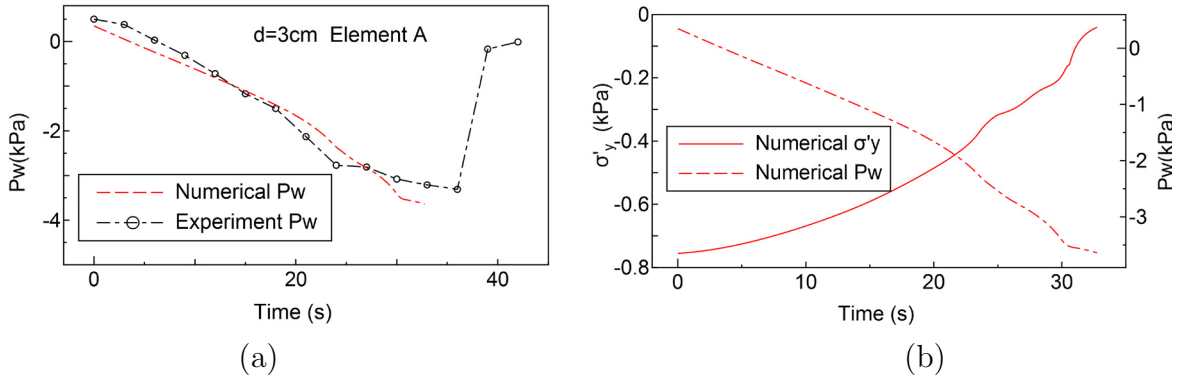


**Figure 4**: (a)The time history of pore water pressure $\boldsymbol{P_w}$; (b)The time history of effective stress $\boldsymbol{\sigma'}$

It is found that, as time goes on, the external vertical force will be transfered and transmited to the base pore water and soil skeleton. As soil effective stress is very small, the pore water pressure becomes the main receiver. But soil effective stress also have to be unloaded, until the moment losing its strength.

In the experiment, the pore water pressure will increase back towards the hydrostatic pressure at the moment of breakout, that beacuse the object will seperate from the soil, the around water will flow into the bottom suddenly, the negative pore water pressure will disappear in a short time. As we know, soil effective stress is difficult to get accurately in model test. But, in numerical simulation, the element effective stress response can be easily presented. So that, from figure 4, we can predict the object will have large displacement by the status of soil skeleton. Not only that, the numerical method also can

describe developing trend of pore water pressure and other variables.
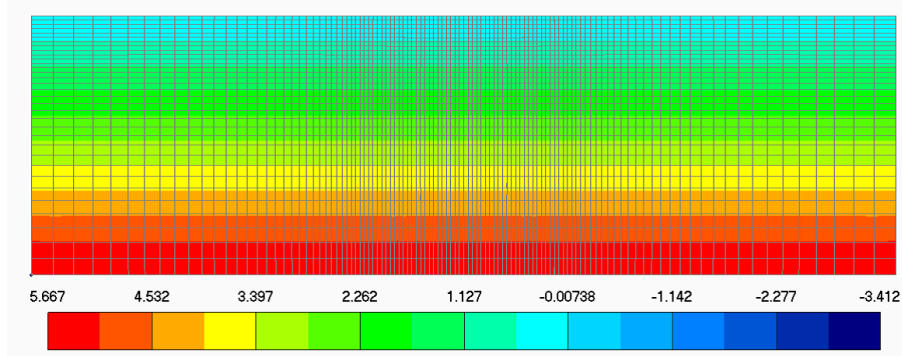


**Figure 5**: The distribution of initial $P_\mathbf{w}$
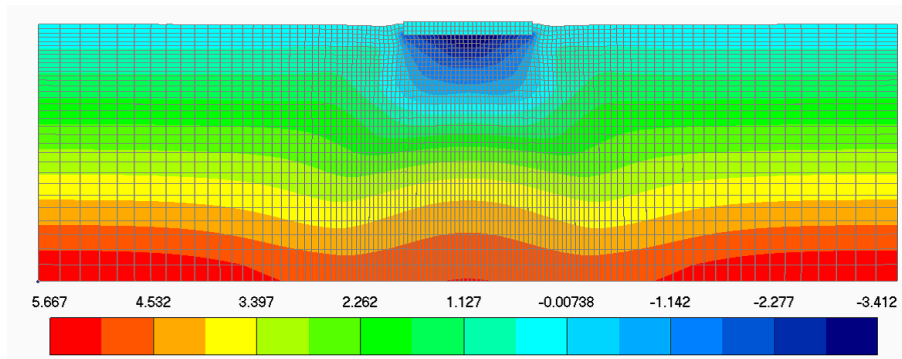


**Figure 6**: The distribution of $P_\mathbf{w}$ when(d=3cm,t=30s)

Figure 5 and figure 6 show the distribution of initial pore water pressure and the pore water pressure when t=30s. The initial pore water pressure equals to the hydrostatic pressure. When t=30s, the area under the object has negative pore water pressure, while the area near the boundary has postive pore water pressure and near the hydrostatic pressure. It can clearly infer that during the pullout process, the vertical pull force induce the negative pore water pressure generated around the object and diffuse to the distance.

### 3.4 Soil deformation

From figure 4, the soil effective stress increase and near to 0 kPa. In figure 7, it shows the ditribution of deviatoric strain in the whole domain when buried depth d=3cm, time t=30s. The deviatoric strain around the object has large value. That means the large soil deformation will happen. In the model test, the soil around the object also has obvious failure area which is shown in figure 8. The numerical simulation and the experiment have the similar phenomenon that the soil around the object has large deformation and the object will has rapid increase in displacement at the beginning of the breakout.

928
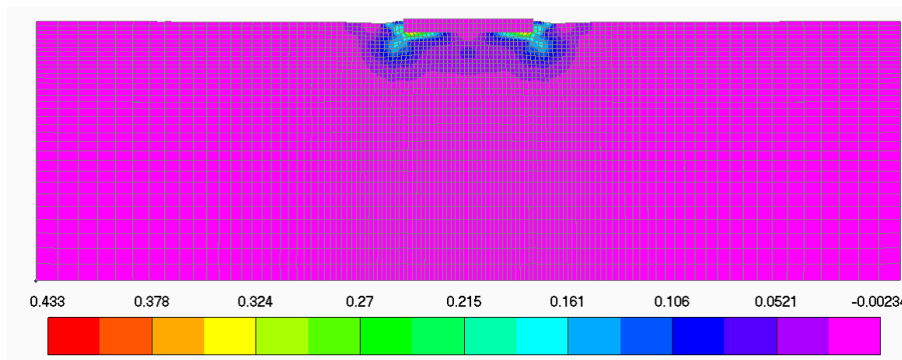
**Figure 7**: The distribution of deviatoric strain (d=3cm,t=30s)
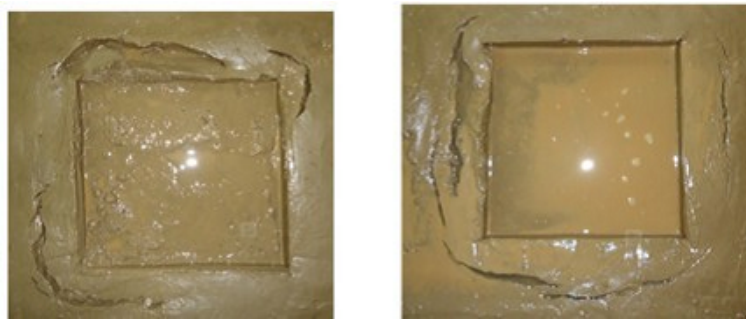


**Figure 8**: The soil around the object after breakout

## 4    CONCLUSIONS

- In this paper, the model tests and numerical simulations are conducted to verify the pullout capacity of the platform legs from saturated silt. The influence and the mechanism of suction force under the legs are explained. From this research, the suction force is mainly composed of negative pore water pressure, to pullout the object, the suction force provide the great mass of resistance.

- During pullout process, the vertical force firstly overcome the object's self weight, then the difference force between vertical force and object effective weight induce the pore water pressure form positive to negative, the effective soil stress will increase near to zero. The partial soil failure around the object occurs, which will lead to large soil deformation and rapid increase of object displacement. In the last, the object will be pulled out.

- In numerical simulation, the porous media theory and finite strain method are used. The time history of the pore water pressure and the displacement are reappeared. It shows the soil large deformation and the rapid increase of displacement very clearly. The model test and numerical simulation have similar phenomenon and results.

The numerical method can be used to predict the pullout resistance in the practical engineering.

**REFERENCES**

[1] Randolph, M. , Cassidy, M. and Gourvenec, S. Challenges of offshore geotechnical engineering. *Proceedings of The 16th International Conference on Soil Mechanics and Geotechnical Engineering.* Vol. 1: 123-176, (2005).

[2] Foda, M.A. , On the extrication of large objects from the ocean bottom (the breakout phenomenon). *Journal of Fluid Mechanics.* Vol. 117: 211-231, (1982).

[3] Finn, W.D. , and Byrne, P.M. The evaluation of the breakout force for a submerged ocean platform. *Proceedings, Fourth Annual Offshore Technology Conference, Houston, Texas..* Vol. 1: 863-868, (1972).

[4] Sawicki, A. , Mierczynski, J. Mechanics of the breakout phenomenon. *Computers and Geotechnics.* Vol. 30: 231-243, (2003).

[5] Purwana, O.A. , Leung, C.F. , Chow, Y.K , and Foo, K.S. Influence of base suction on extraction of jack-up spudcans. *Geotechnique.* Vol. 55(10): 741-753, (2005).

[6] Zhou, X.X. , Chow, Y.K. and Leung, C.F. Numerical modeling of breakout process of objects lying on the seabed surface. *Computers and Geotechnics.* Vol. 35: 686-702, (2008).

[7] Mei, C.C. , Yeung, R.W. and Liu K.F. Lifting of a large object from a porous seabed. *Journal of Fluid Mechanics.* Vol. 152: 203-215, (1985).

[8] Chen, R. ,Gaudin. C. and Cassidy, M.J. Investigation of the vertical uplift capacity of deep water mudmats in clay. *Canadian Geotechnical Journal.* Vol. 49(7): 853-865, (2012).

[9] Al-Shamrani, M. A. Finite Element Analysis of Breakout Force of Objects Embedded in Sea Bottom. *Civil Engineering Research Magazine, Al-Azhar University, Cairo, Egypt.* Vol. 19(2): 288-304, (1997).

[10] Uzuoka, R. and Borja, R.I. Dynamics of unsaturated poroelastic solids at finite strain. *Internal Journal for Numerical and Analytical Methods in Geomechanics.* Vol. 36: 1535—1573, (2012).